# Thermally-Accessible Lattice Strain and Local Pseudo Jahn-Teller Distortion in Various Dimensional $Cu^{II}$-$M^{III}$ Bimetallic Cyanide-Bridged Assemblies

Takashiro Akitsu*,[a] Yasuaki Einaga[a] and Kenji Yoza[b]

[a]*Department of Chemistry, Faculty of Science and Technology, Keio University, 3-14-1 Hiyoshi, Kohoku-ku, Yokohama, Kanagawa 223-8522, Japan*

[b]*Brucker AXS K.K. 3-9-A Moriya-cho, Kanagawa-ku, Yokohama, Kanagawa 221-0022, Japan*

**Abstract:** Cocrystals of one-dimensional cyanide-bridged $Cu^{II}$-$Cr^{III}$ or $Cu^{II}$-$Co^{III}$ bimetallic assemblies and mononuclear $Cu^{II}$ complexes, $[Cu(chxn)_2]_3[M(CN)_6]_2{\cdot}4H_2O$ (chxn = *trans*-cyclohexane-(*1R*,*2R*)-diamine; M = Cr for **1** and Co for **2**), and two-dimensional cyanide-bridged $Cu^{II}$-$Fe^{III}$ bimetallic assembly, $[Cu(N\text{-Eten})_2]_3[Fe(CN)_6]_2{\cdot}4H_2O$ (*N*-Eten = *N*-ethylethylenediamine) (**3**), were prepared and characterized structurally. Crystal structures were determined at 263 and 100 K for **1** and **2**, while at 299 and 100 K for **3**. Thermally-accessible lattice strain resulted in decreasing cell volume of 1.66, 1.06, and 4.1 % for **1**-**3**, respectively. Large thermally-accessible structural change but small pseudo Jahn-Teller elongation at constant temperature could be found in both the long chain of the ladder structure for **3** and the monocuclear $Cu^{II}$ moieties for **1** and **2**. In addition, novel mixing of ferromagnetic and antiferromagnetic interactions at low temperature was observed for **3**. The correlations between dimensionality of cyanide-bridges and thermally-accessible structural changes distortion associated with Jahn-Teller distortion are also discussed by comparing with several known systems.

**Keywords:** X-ray crystallography, copper, Jahn-Teller distortion, temperature, cyanide-bridged, dimensionality.

## INTRODUCTION

In recent years, hexacyanometalates have been employed as important building blocks for designing cyanide-bridged bimetallic assemblies, which can afford various dimensionality (1D chains, 2D ladders, and 3D networks) [1, 2]. In particular, multi-functional cyanide-bridged molecule-based magnetic materials [3, 4] such as photomagnets [5-8], chiral magnets [9-13], and magnetic conductors [14] have attracted much attention from potential applications functional devices. Molecular design including electronic functions of cyanide-bridged metal complexes is still challenging task in the field of crystal engineering of organic-inorganic frameworks or coordination polymers.

Interestingly, it was reported that some Prussian blue analogues, ($Zn^{II}$ or $Cd^{II}$)$[Pt^{IV}(CN)_6]{\cdot}xH_2O$ and $Er^{III}[Co^{III}(CN)_6]{\cdot}4H_2O$ [15, 16], exhibited negative thermal expansion [17]. In contrast to usual phonon density of states and population of higher energy vibrational modes as a function of temperature, negative thermal expansion occurs for certain materials for which the underlying thermal expansion of chemical bonds may become dominated by other factors which tend to lead to a contraction in volume in certain temperature ranges for complicated solid state systems. Thus, structural distortion of cyanide-bridged complexes may be one of the important factors for photo- or thermally-controllable crystalline materials.

In this context, we focused on flexibility and distortion of crystal structures involving $Cu^{II}$ moieties showing (pseudo) Jahn-Teller effect [18, 19]. In general, six-coordinated $Cu^{II}$ complexes in $O_h$ symmetry are subject to a strong $E \times \varepsilon$ coupling described by wrapped Mexican hat potential energy surface [20-24]. Three energy minima correspond to the orientation of distorted octahedral coordination environment and the frequency of transition between energy minima of dynamic equilibrium. The populations of the differently elongated octahedral may be temperature dependent. Ligand field strength and bond lengths of axial ligands decide that magnetic orbital of $Cu^{II}$ ion is $d_{x2-y2}$ or $d_{z2}$ [22] (Fig. **1**). Additionally, configuration interaction between $3d_{z2}$ and 4s orbitals mixing is also subjected to tetrahedral as well as tetragonal distortion of $Cu^{II}$ coordination environment [25-27]. However, temperature dependence of (pseudo) Jahn-Teller distortion of $Cu^{II}$ moieties has not been investigated in view of dimensions of cyanide-bridges so far [28-31].

In this study, we investigate spectroscopic and magnetic properties and crystal structures at two different temperatures for cocrystals of one-dimensional cyanide-bridged $Cu^{II}$-$Cr^{III}$ and $Cu^{II}$-$Co^{III}$ bimetallic assemblies and mononuclear $Cu^{II}$ complexes, $[Cu(chxn)_2]_3[M(CN)_6]_2{\cdot}4H_2O$ (chxn = *trans*-cyclohexane-(*1R*,*2R*)-diamine; M = Cr for **1** and Co for **2**) and two-dimensional cyanide-bridged $Cu^{II}$-$Fe^{III}$ bimetallic assembly, $[Cu(N\text{-Eten})_2]_3[Fe(CN)_6]_2{\cdot}4H_2O$ (*N*-Eten = *N*-ethylethylenediamine) (**3**).

## EXPERIMENTAL SECTION

### Materials

All reagents and solvents were obtained from commercial sources and used without further purification. Caution: Transition metal perchlorates are potentially explosive and should be prepared in small quantities and with care! Cyanide compounds are potentially dangerous for health.

*Address correspondence to these authors at the Department of Chemistry, Faculty of Science and Technology, Keio University, 3-14-1 Hiyoshi, Kohoku-ku, Yokohama, Kanagawa 223-8522, Japan;
E-mail: akitsu@chem.keio.ac.jp

1874-0987/08 

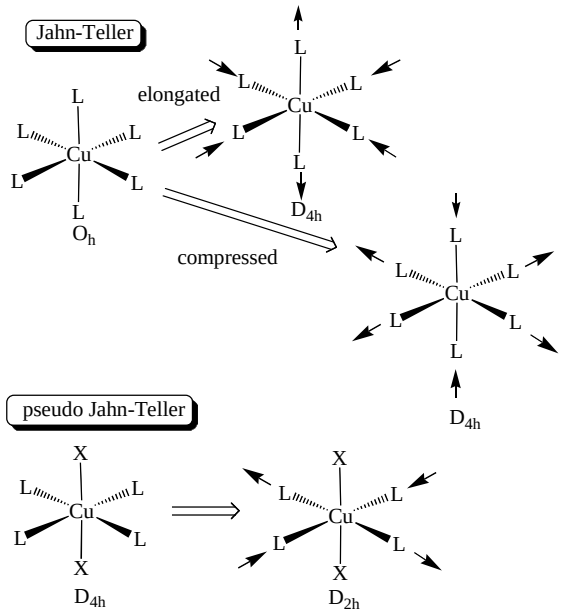


**Fig. (1).** Schematic representation of typical Jahn-Teller ($O_h$) and pseudo Jahn-Teller ($D_{4h}$) distortion of $Cu^{II}$ complexes.

### Preparation of $[Cu(chxn)_2]_3[Cr(CN)_6]_2 \cdot 4H_2O$ (1)

Blue prismatic crystals of new compound **1** were obtained according to the literature procedure by using $K_3[Cr(CN)_6]$ [9]. Anal. calcd for $C_{48}H_{92}Cr_2Cu_3N_{24}O_4$: C, 42.27; H, 6.80; N, 24.64. Found: C, 42.22; H, 6.38; N, 24.51. IR ($cm^{-1}$, KBr): 457(s), 568(s), 681(s), 822(s), 1039(s), 1124(s), 1590(s), 2124(s) (C≡N), 2856(s), 2933(s), 3149(s), 3266(s), 325(s), 3444(s). Diffuse reflectance electronic spectrum ($cm^{-1}$): 19100 (d-d), 28900 (π–π*). XPS (eV): C 1s 284, N 1s 397, O 1s 512, Cr $2p_{1/2}$ 580.2, Cu $2p_{1/2}$ 935.8, Cu $2p_{3/2}$ 955.0. m.p. 673 K (decomposition). XRD(2θ(˚), CuKα): 16.7, 21.6, 26.3, 30.5, 44.8.

### Preparation of $[Cu(chxn)_2]_3[Co(CN)_6]_2 \cdot 4H_2O$ (2)

Blue prismatic crystals of new compound **2** were obtained according to the literature procedure by using $K_3[Co(CN)_6]$ [9]. Anal. calcd for $C_{48}H_{92}Co_2Cu_3N_{24}O_4$: C, 41.84; H, 6.73; N, 24.40. Found: C, 42.26; H, 6.57; N, 24.24. IR ($cm^{-1}$, KBr): 553(s), 681(s), 824(s), 1042(s), 1126(s), 1590(s), 2117(s) (C≡N), 2856(s), 2931(s), 3140(s), 3319(s), 3430(s). Diffuse reflectance electronic spectrum ($cm^{-1}$): 17600 (d-d), 23400 (π–π*), 25600 (CT). XPS (eV): C 1s 284, N 1s 397, O 1s 512, Co $2p_{1/2}$ 720.2, Co $2p_{3/2}$ 784.5, Cu $2p_{1/2}$ 936.6, Cu $2p_{3/2}$ 955.9. m.p. 673 K (decomposition). XRD(2θ(˚), CuKα): 16.7, 21.6, 26.3, 30.5, 44.8.

### Preparation of $[Cu(N\text{-Eten})_2]_3[Fe(CN)_6]_2 \cdot 4H_2O$ (3)

Blue prismatic crystals of **3** were grown according to the literature procedure of an analogous complex with slight modification [32]. Anal. Calcd for $C_{36}H_{80}N_{24}Cu_3Fe_2O_4$: C, 35.57, H, 6.63, N, 27.66. Found: C, 35.57, H, 6.63, N, 27.66. IR ($cm^{-1}$, KBr): 585(w), 636(w), 873(w), 986(m), 1101(m), 1120(s), 1282(w), 1398(w), 1465(m), 1601(m), 2104(s) (C≡N), 2916(m), 2980(m), 3201(sh), 3269(s), 3327(2), 3470(s). Diffuse reflectance electronic spectrum ($cm^{-1}$): 17600 (d-d), 23400 (CT).

### Physical Measurements

Elemental analyses (C, H, N) were carried out an Elementar Vario EL analyzer at Keio University. Infrared spectra were recorded as KBr pellets on a JASCO FT-IR 660 plus and BIORAD FTS-60A spectrophotometer in the range of 4000-400 $cm^{-1}$ at 298 K. Diffuse reflectance electronic spectra were measured on a JASCO V-560 spectrophotometer equipped with an integrating sphere in the range of 850-220 nm at 298 K. Circular dichroism (CD) and magnetic circular dichroism (MCD) under 1.5 T at 298 K were recorded as KBr pellets on a JASCO J-720WI specropolarimater in the range of 900-200 nm. Thermal analysis was performed on a SHIMADZU DSC-60 differential scanning calorimeter (DSC), where the heating rate was 10 $Kmin^{-1}$ in the range of 313-673 K. Powder XRD patterns were obtained by a Rigaku RAD-C diffractometer with CuKα radiation. The magnetic properties were investigated with a Quantum Design MPMS-XL and 5S superconducting quantum interference device magnetometer (SQUID) at an applied field 0.5 T in a temperature range 5-300 K. Powder samples were measured in a pharmaceutical cellulose capsule. The apparatus signals and the diamagnetic corrections were evaluated from Pascal's constants. X-ray photoelectron spectra (XPS) were recorded with a JEOL JPS-9000MX at 298 K. Powder samples were pressed as pellets and put under UHV to reach the $10^{-8}$ Pa range. The nonmonochromatized Mg Kα source was used at 10 kV and 10 mA, as a flood gun to compensate for the nonconductive samples. The binding energy of the spectra was calibrated in relation to the C 1s binging energy (284.0 eV), which was applied as an internal standard. The XPS data have been deposited to the database of *Surface Science Spectra* (American Vacuum Society).

### X-Ray Crystallography

Blue prismatic single crystals of **1** with 0.10 x 0.08 x 0.01 $mm^3$ size, **2** with 0.10 x 0.05 x 0.05 $mm^3$ size, and **3** of 0.90 x 0.70 x 0.10 $mm^3$ size were glued on the tip of a glass fiber. The composition of well-grown single crystals of **1** and **2** measured were $[Cu(chxn)_2]_3[M(CN)_6]_2 \cdot 5H_2O$. The diffraction data for **1** and **2** were collected on a Bruker SMART APEXII CCD diffractometer at 100 K and 263 K, while **3** were collected on a Bruker SMART APEX CCD diffractometer at 100 K and 299 K, with graphite monochromated MoKα radiation (λ = 0.71073 Å). Intensities were collected by the ω scan technique. The data were corrected for Lorentz and polarization effects, but absorption correction could not be applied for **3**. The structures were solved by direct methods (SIR 92) and expanded by Fourier techniques. The structure was refined on $F^2$ anisotropically for non-hydrogen atoms by full-matrix least-squares methods (SHELXL-97 [33]). All the hydrogen atoms were located by geometrically calculated positions and all were refined by using riding model.

## RESULTS AND DISCUSSION

### Crystal Structures

As shown in Tables **1-3** and Fig. (**2**), both **1** and **2** are isostructural essentially and similar to the $Fe^{III}$ analogues reported [9]. Both **1** and **2** are cocrystals containing separated mononuclear $[Cu^{II}(chxn)_2(H_2O)_2]^{2+}$ moieties and one-

dimensional zigzag cyanide-bridged bimetallic assemblies made up of alternating $[Cu^{II}(chxn)_2]^{2+}$ cations and $[M^{III}(CN)_6]^{3-}$ anions, ---Cu1---M1---Cu2---M2---Cu1'---, along the crystallographic *c* axis. Bond distances and angles in $[Cu^{II}L_2]^{2+}$ cations are in agreement with that of the corresponding mononuclear $Cu^{II}$ complex [34]. The *R,R*-enantiomers of chiral ligands gave rise to a λ-conformation as the resulting complexes. Hydrogen bonded (omitted from the Tables because of less importance) lattice waters (O3, O4, and O5) are also involved in the crystals normally.

The influence of temperature upon the three different Jahn-Teller active $Cu^{II}$ sites has been investigated in the crystals of **1** and **2**. Overall crystal structures at 263 K and 100 K are in agreement with each other without structural phase transitions. All the non-hydrogen atoms could be refined using anisotropic thermal displacement parameters without disorder or other abnormal features. The cell volume decreased by only 1.66 % and 1.06 % for **1** and **2**, respectively. The most remarkable direction was the *b* axis which decreased by 1.18 % for **1**.

As a conventional index of Jahn-Teller distortion, *T*, which is the ratio of equatorial Cu-X bond distances / axial Cu-X bond distances [18], the degree of distortion around Cu1, Cu2, and Cu3 (Fig. **2**) can be described as $T = 0.761$, 0.748, and 0.816 for **1** at 263 K, $T = 0.778$, 0.757, and 0.830 for **1** at 100 K, $T = 0.747$, 0.736, and 0.813 for **2** at 263 K, and $T = 0.760$, 0.743, and 0.826 for **2** at 100 K, respectively. Differences between **1** and **2** are attributed to only ionic radii of $Cr^{III}$ and $Co^{III}$. It should be noted that the $Cu^{II}$ moieties of one-dimensional chains are largely distorted from regular octahedral environment by Jahn-Teller effect at both 263 K and 100 K, while the mononuclear $Cu^{II}$ moieties showing small Jahn-Teller elongation exhibit large structural changes by changing temperature between 263 K and 100 K.

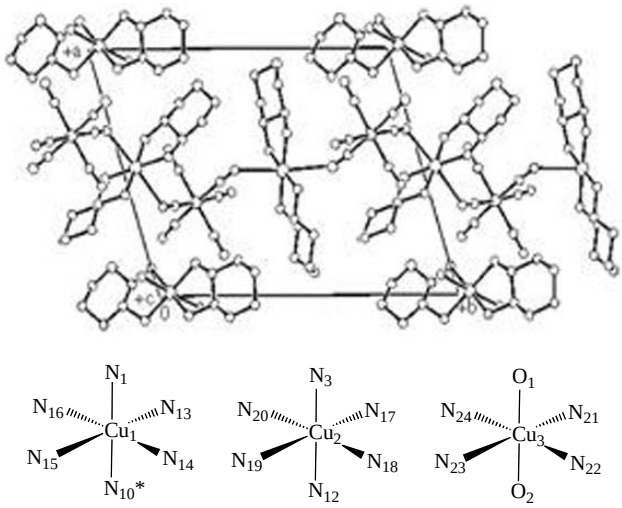


**Fig. (2).** [above] Molecular packing scheme of **1** and **2** drawn as irreducible cell for clarity. [below] Cu coordination environment of **1** and **2**.

As shown in Tables **4** and **5**, and Fig. (**3**), **3** are isostructural essentially and also similar to the $Co^{III}$ analogues reported [32]. Self-assembling complexes consist of $[M(CN)_6]^{3-}$ and $[CuL_2]^{2+}$ the ratio of 2:3 and water molecules as solvents to satisfy neutral charges. Two-dimensional zigzag networks of interchain cyanide-bridges of -Fe1-CN-Cu1-NC-Fe2- running in the *ac* plane and long cyanide-bridging chains of -Fe2-CN-Cu2-NC-Fe2- along the crystallographic *a* axis are formed in the crystals. Irrespective of bridging cyanides or terminal ones, no remarkable deviation is observed in structural features about cyanides [35-41], and *cis*-C-M-C and *trans*-C-M-C bond angles are close to 90˚ and 180˚, respectively. Indeed, the structures of coordinating cyanides are in agreement with that of being involved by π-backdonation from the filled $d_\pi$ orbitals of metals to the empty π* orbitals of cyanides.

Therefore, strictly speaking, orthogonality of the magnetic orbitals to be pure ferromagnetic interactions was broken around superexchanging cyanide-bridges (*vide infra*).

Based on variable temperature crystallography of **3**, the *T* values of Cu1 (interchain bridges) are $T = 0.782$ and 0.782 at 299 K and 100 K, and Cu2 (intra-long-chains along the *a* axis) are $T = 0.811$ and 0.817 at 299 K and 100 K, respectively. Although the Cu2 sites are less distorted from regular octahedral than Cu1 ones at each temperature, the Cu2 sites exhibit larger temperature dependence around coordination environment associated with Jahn-Teller effect. The tendency of less distorted $Cu^{II}$ moieties at each temperature exhibits large changes at low temperature is similar to that of the mononuclear $Cu^{II}$ moieties in **1** and **2**.

## Electronic and CD Spectra

As shown in Fig. (**4**), the solid state CD spectra exhibited positive peak at 19200 $cm^{-1}$ and negative peaks at 16700 $cm^{-1}$ and 33000 $cm^{-1}$ for **1**, and positive peak at 19100 $cm^{-1}$ and 27200 $cm^{-1}$ (shoulder) and a negative peak at 31400$cm^{-1}$ for **2**. The assignment of Cotton effect for $[Cu^{II}(chxn)_2]_3[Fe^{III}(CN)_6]_2{\cdot}nH_2O$ (**Cu-Fe**) was reported by Coronado and coworkers is as follows [9, 10]: positive d-d peak at 14500 $cm^{-1}$, positive CT peak at 18900 $cm^{-1}$, and negative CT peak at 28600 $cm^{-1}$. MCD spectra under 1.5 T (as reference and not shown, because characteristic magnetic interaction could not be measured at room temperature) exhibited positive peak at 19300 $cm^{-1}$ and negative peaks at 16600 $cm^{-1}$ and 34000 $cm^{-1}$ for **1** and exhibited at 19100 $cm^{-1}$, 27000 $cm^{-1}$ (shoulder), and a negative peak at 31600 $cm^{-1}$ for **2**. In this way, we also measured diffuse reflectance spectra of both mononuclear components and bimetallic assemblies by metal-substitution of $Cr^{III}$, $Co^{III}$, and $Fe^{III}$. The spectra exhibit a broad d-d band of $Cu^{II}$ chromophores at 19100, 19100, 19800, and 19400 $cm^{-1}$ for $[Cu(chxn)_2](ClO_4)_2$, **1**, **2**, and **Cu-Fe**, respectively. In addition, the spectra show π–π* bands at 28900, 26000, and 26500 $cm^{-1}$ for **1**, **2**, and **Cu-Fe**, respectively, and charge transfer (CT) bands (shoulders) at 25600 and 22900 $cm^{-1}$ for **2** and **Cu-Fe**, respectively.

On the other hand, as shown in Fig. (**5**), **3** exhibits a d-d band at 17600$cm^{-1}$ and a π–π* band at 23400 $cm^{-1}$, whereas the analogous $[Cu(N\text{-Eten})_2]_3[Co(CN)_6]_2{\cdot}4H_2O$ complex [32] exhibits a d-d band at 17500 $cm^{-1}$, and both compounds show continuously intense CT bands in the UV region more than 32000 $cm^{-1}$. Fig. (**5**) also exhibits mononuclear components such as a peak at 19300 $cm^{-1}$ for $[Cu(N\text{-Eten})_2](ClO_4)_2$, at 23700 and 28700 $cm^{-1}$ (CT) and 33400 and 33900 $cm^{-1}$ for $K_3[Fe(CN)_6]$, and peaks at 26100 $cm^{-1}$ (CT), and 32300 and 38800 $cm^{-1}$ for $K_3[Co(CN)_6]$.

**Table 1. Crystallographic Data for 1 and 2 at 263 and 100 K**

| | **1** | | **2** | |
|---|---|---|---|---|
| **T (K)** | **263** | **100** | **263** | **100** |
| Formula | $C_{48}H_{88}Cr_2Cu_3N_{24}O_5$ | $C_{48}H_{88}Cr_2Cu_3N_{24}O_5$ | $C_{48}H_{88}Co_2Cu_3N_{24}O_5$ | $C_{48}H_{88}Co_2Cu_3N_{24}O_5$ |
| Fw | 1376.04 | 1376.04 | 1389.90 | 1389.90 |
| Crystal system | triclinic | triclinic | triclinic | triclinic |
| Space group | *P1* | *P1* | *P1* | *P1* |
| *a* (Å) | 8.519(4) | 8.5093(6) | 8.366(2) | 8.3431(5) |
| *b* (Å) | 12.777(6) | 12.6258(9) | 12.700(2) | 12.6316(8) |
| *c* (Å) | 16.201(8) | 16.103(1) | 16.086(3) | 16.020(1) |
| $\alpha$(°) | 105.142(6) | 104.571(1) | 105.750(2) | 105.418(1) |
| $\beta$(°) | 98.326(7) | 98.549(1) | 98.760(2) | 99.130(1) |
| $\gamma$(°) | 97.379(7) | 97.205(1) | 96.119(2) | 95.743(1) |
| *V* (Å$^3$) | 1659(1) | 1631.7(2) | 1605.9(5) | 1588.9(2) |
| *Z* | 1 | 1 | 1 | 1 |
| $\rho_{calc}$ (g/cm$^3$) | 1.378 | 1.400 | 1.437 | 1.453 |
| $\mu$(mm$^{-1}$) | 1.323 | 1.345 | 1.544 | 1.561 |
| *F(000)* | 719 | 719 | 725 | 725 |
| Reflections collected | 8141 | 8114 | 5923 | 7714 |
| Unique reflections | 5152 [R(int) = 0.0278] | 7122 [R(int) = 0.0178] | 7834 [R(int) = 0.0194] | 6946 [R(int) = 0.0170] |
| Parameters | 751 | 751 | 739 | 739 |
| Goodness of fit | 0.952 | 1.004 | 1.041 | 1.007 |
| $R_1$ [$I > 2\sigma(I)$] | 0.0539 | 0.0377 | 0.0404 | 0.0341 |
| $wR_2$ (all data) | 0.1320 | 0.0856 | 0.0867 | 0.0775 |
| Flack parameter | -0.01(2) | -0.01(1) | -0.02(2) | -0.03(1) |

**Table 2. Selected Bond Distances (Å) for 1 and 2 at 263 and 100 K**

| | **1 (263 K)** | **1 (100 K)** | **2 (263 K)** | **2 (100 K)** |
|---|---|---|---|---|
| Cu1-N1 | 2.65(1) | 2.587(5) | 2.685(7) | 2.629(5) |
| Cu1-N10$^i$ | 2.65(1) | 2.593(5) | 2.675(7) | 2.652(5) |
| Cu1-N13 | 2.005(8) | 2.006(4) | 1.993(6) | 2.003(4) |
| Cu1-N14 | 2.024(8) | 2.022(4) | 2.016(6) | 2.018(4) |
| Cu1-N15 | 2.006(9) | 2.010(5) | 1.995(6) | 1.994(4) |
| Cu1-N16 | 2.019(8) | 2.026(4) | 2.003(5) | 2.018(4) |
| Cu2-N3 | 2.73(1) | 2.668(5) | 2.795(7) | 2.746(5) |
| Cu2-N12 | 2.62(1) | 2.639(5) | 2.640(7) | 2.651(5) |
| Cu2-N17 | 1.986(9) | 2.001(5) | 2.014(6) | 2.017(4) |
| Cu2-N18 | 2.025(8) | 2.028(4) | 1.977(6) | 1.989(4) |
| Cu2-N19 | 1.996(9) | 1.993(5) | 2.021(6) | 2.021(4) |
| Cu2-N20 | 2.010(8) | 2.012(4) | 1.992(6) | 1.995(4) |
| Cu3-O1 | 2.461(9) | 2.430(4) | 2.474(4) | 2.441(4) |
| Cu3-O2 | 2.492(9) | 2.450(4) | 2.494(4) | 2.457(4) |
| Cu3-N21 | 2.028(7) | 2.034(4) | 2.006(6) | 2.019(4) |
| Cu3-N22 | 2.024(8) | 2.017(5) | 2.036(6) | 2.037(4) |
| Cu3-N23 | 2.028(8) | 2.028(4) | 2.025(6) | 2.019(4) |
| Cu3-N24 | 2.006(9) | 2.025(5) | 2.012(7) | 2.022(4) |

[Symmetry code: (i) 1+x, y, 1+z].

**Table 3. Selected Bond Angles (˚) for 1 and 2 at 263 and 100 K**

| | 1 (263 K) | 1 (100 K) | 2 (263 K) | 2 (100 K) |
|---|---|---|---|---|
| N1-Cu1-N10$^{i}$ | 176.6(3) | 176.9(2) | 175.9(2) | 176.1(2) |
| N13-Cu1-N15 | 177.5(5) | 177.0(2) | 176.4(3) | 176.4(2) |
| N14-Cu1-N16 | 177.1(5) | 177.4(2) | 177.3(3) | 177.1(2) |
| N1-Cu1-N13 | 94.4(3) | 94.1(2) | 95.7(2) | 95.5(2) |
| N1-Cu1-N14 | 88.7(3) | 88.9(2) | 90.3(2) | 89.5(2) |
| N1-Cu1-N15 | 88.0(3) | 88.9(2) | 87.9(3) | 88.1(2) |
| N1-Cu1-N16 | 88.5(3) | 88.6(2) | 87.1(2) | 87.7(2) |
| N10$^{i}$-Cu1-N13 | 87.4(3) | 87.6(2) | 85.8(2) | 86.5(2) |
| N10$^{i}$-Cu1-N14 | 94.3(3) | 93.8(2) | 93.6(2) | 94.0(2) |
| N10$^{i}$-Cu1-N15 | 90.2(3) | 89.5(2) | 90.7(3) | 89.9(2) |
| N10$^{i}$-Cu1-N16 | 88.5(3) | 88.7(2) | 89.0(2) | 88.8(2) |
| N3-Cu2-N12 | 175.2(4) | 174.9(2) | 178.5(4) | 173.9(2) |
| N17-Cu2-N19 | 177.3(5) | 178.4(2) | 176.6(3) | 177.8(2) |
| N18-Cu2-N20 | 176.2(4) | 177.4(2) | 177.8(3) | 177.9(2) |
| N3-Cu2-N17 | 87.4(4) | 87.0(2) | 86.6(2) | 86.5(2) |
| N3-Cu2-N18 | 88.4(3) | 90.8(2) | 92.8(2) | 93.1(2) |
| N3-Cu2-N19 | 93.0(4) | 93.5(2) | 93.0(3) | 91.2(2) |
| N3-Cu2-N20 | 88.0(3) | 87.2(2) | 86.1(2) | 85.6(2) |
| N12-Cu2-N17 | 94.2(4) | 96.1(2) | 89.9(2) | 89.5(2) |
| N12-Cu2-N18 | 96.2(3) | 93.5(2) | 83.3(3) | 82.0(2) |
| N12-Cu2-N19 | 85.2(4) | 83.3(2) | 93.0(3) | 91.2(2) |
| N12-Cu2-N20 | 87.4(3) | 88.5(2) | 97.6(3) | 99.2(2) |
| O1-Cu3-O2 | 179.0(4) | 178.8(2) | 179.2(2) | 178.8(2) |
| N21-Cu3-N23 | 178.3(4) | 179.4(2) | 178.5(4) | 178.4(2) |
| N22-Cu3-N24 | 177.9(5) | 178.3(2) | 178.8(3) | 179.0(2) |
| O1-Cu3-N21 | 90.6(3) | 91.3(2) | 90.4(2) | 92.0(2) |
| O1-Cu3-N22 | 92.3(4) | 92.9(2) | 89.6(2) | 91.4(2) |
| O1-Cu3-N23 | 89.9(3) | 89.2(2) | 90.5(2) | 89.4(2) |
| O1-Cu3-N24 | 89.4(4) | 88.7(2) | 90.7(2) | 89.3(2) |
| O2-Cu3-N21 | 90.2(3) | 89.9(2) | 88.8(2) | 88.3(2) |
| O2-Cu3-N22 | 87.3(4) | 87.2(2) | 90.4(2) | 89.8(2) |
| O2-Cu3-N23 | 89.3(3) | 89.6(2) | 90.2(2) | 90.4(2) |
| O2-Cu3-N24 | 90.9(4) | 91.3(2) | 89.4(2) | 89.5(2) |

[Symmetry code: (i) 1+x, y, 1+z].

**Table 4. Crystallographic Data for 3 at 299 and 100 K**

| | 3 | |
|---|---|---|
| **T (K)** | **299** | **100** |
| Formula | $C_{36}H_{80}Cu_3Fe_2N_{24}O_4$ | $C_{36}H_{80}Cu_3Fe_2N_{24}O_4$ |
| Fw | 1215.59 | 1215.59 |
| Crystal system | triclinic | triclinic |
| Space group | *P-1* | *P-1* |
| *a* (Å) | 10.026(2) | 9.922(4) |
| *b* (Å) | 11.976(2) | 11.779(5) |
| *c* (Å) | 12.066(2) | 11.877(5) |
| $\alpha$ (˚) | 78.210(3) | 78.195(7) |
| $\beta$ (˚) | 83.089(3) | 83.354(6) |

**(Table 4). Contd…..**

| | 3 | |
|---|---|---|
| **T (K)** | **299** | **100** |
| $\gamma$(°) | 88.928(3) | 88.992(7) |
| $V$ (Å$^3$) | 1407.9(4) | 1350(1) |
| $Z$ | 1 | 1 |
| $\rho_{calc}$ (g/cm$^3$) | 1.434 | 1.496 |
| $\mu$(mm$^{-1}$) | 1.675 | 1.748 |
| *F(000)* | 635 | 635 |
| Reflections collected | 6829 | 6560 |
| Unique reflections | 5031 [R(int) = 0.0189] | 4822 [R(int) = 0.0221] |
| Parameters | 317 | 317 |
| Goodness of fit | 1.090 | 1.036 |
| $R_1$ [$I > 2\sigma(I)$] | 0.0398 | 0.0552 |
| $wR_2$ (all data) | 0.1190 | 0.1507 |

**Table 5. Selected Bond Distances (Å) and Angles (°) for 3 at 299 K and 100 K**

| | 3 (299 K) | 3 (100 K) | | 3 (299 K) | 3 (100 K) |
|---|---|---|---|---|---|
| Cu1-N9 | 1.994(2) | 1.991(3) | Fe1-C3 | 1.941(3) | 1.930(3) |
| Cu1-N7 | 2.015(2) | 2.009(3) | Fe2-C6 | 1.934(2) | 1.919(3) |
| Cu1-N8 | 2.047(2) | 2.026(3) | Fe2-C5 | 1.934(3) | 1.925(3) |
| Cu1-N10 | 2.067(2) | 2.044(3) | Fe2-C4 | 1.933(3) | 1.935(3) |
| Cu1-N1 | 2.353(2) | 2.312(3) | N1-C1 | 1.152(3) | 1.154(4) |
| Cu1-N4 | 2.843(3) | 2.819(3) | N2-C2 | 1.146(4) | 1.133(4) |
| Cu2-N11 | 2.024(2) | 2.011(3 | N3-C3 | 1.130(4) | 1.137(5) |
| Cu2-N12 | 2.062(2) | 2.045(3) | N4-C4 | 1.155(4) | 1.141(4) |
| Cu2-N6 | 2.519(2) | 2.477(3) | N5-C5 | 1.143(4) | 1.143(4) |
| Fe1-C1 | 1.927(2) | 1.918(3) | N6-C6 | 1.140(3) | 1.147(4) |
| Fe1-C2 | 1.941(3) | 1.935(3) | | | |
| N9-Cu1-N7 | 168.1(1) | 168.2(1) | C1$^{ii}$-Fe1-C2 | 90.1(1) | 90.4(1) |
| N9-Cu1-N8 | 93.1(1) | 92.3(1) | C1-Fe1-C2 | 89.9(1) | 89.6(1) |
| N7-Cu1-N8 | 84.1(1) | 84.5(1) | C1-Fe1-C3 | 88.4(1) | 88.3(1) |
| N9-Cu1-N10 | 85.10(9) | 85.1(1) | C2-Fe1-C3 | 90.2(1) | 89.9(1) |
| N7-Cu1-N10 | 96.35(9) | 96.6(1) | C1-Fe1-C3$^{ii}$ | 91.6(1) | 91.7(1) |
| N8-Cu1-N10 | 172.6(1) | 172.4(1) | C2-Fe1-C3$^{ii}$ | 89.8(1) | 90.1(1) |
| N9-Cu1-N1 | 95.78(9) | 95.1(1) | C6-Fe2-C5$^{iii}$ | 93.6(1) | 93.7(1) |
| N7-Cu1-N1 | 96.01(9) | 96.5(1) | C6-Fe2-C5 | 86.4(1) | 86.3(1) |
| N8-Cu1-N1 | 97.2(1) | 97.5(1) | C6-Fe2-C4$^{iii}$ | 90.8(1) | 90.6(1) |
| N10-Cu1-N1 | 90.12(9) | 89.9(1) | C5-Fe2-C4$^{iii}$ | 91.1(1) | 91.2(1) |
| N11-Cu2-N12 | 84.40(9) | 84.4(1) | C6-Fe2-C4 | 89.2(1) | 89.4(1) |
| N11$^{i}$-Cu2-N12 | 95.60(9) | 95.6(1) | C5-Fe2-C4 | 88.8(1) | 88.8(1) |

[Symmetry codes: (i) –x, -y, -z+2; (ii) –x+2, -y+1, -z+1; (iii) –x+1, -y, -z+2].

Although it is difficult to resolve each band of mixed chromophores reasonably, spectral features do reflect ligand field bands of *trans*-[Cu$^{II}$N$_4$X$_2$] chromophores and spectral shift caused by cyanide complexes as the axial ligands. It is well established that π–π* bands appear at 23500 cm$^{-1}$ ($\sigma t_{1u}$-$t_{2g}$Fe), 33000 cm$^{-1}$ ($\pi t_{2u}$-$t_{2g}$Fe), 38460 cm$^{-1}$ ($\pi t_{1u}$-$t_{2g}\pi^*$),

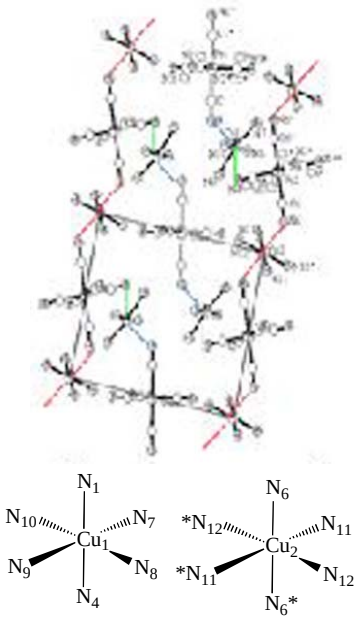


**Fig. (3).** [above] Molecular packing scheme of **3** drawn as irreducible cell for clarity. [below] Cu coordination environment of **3**.

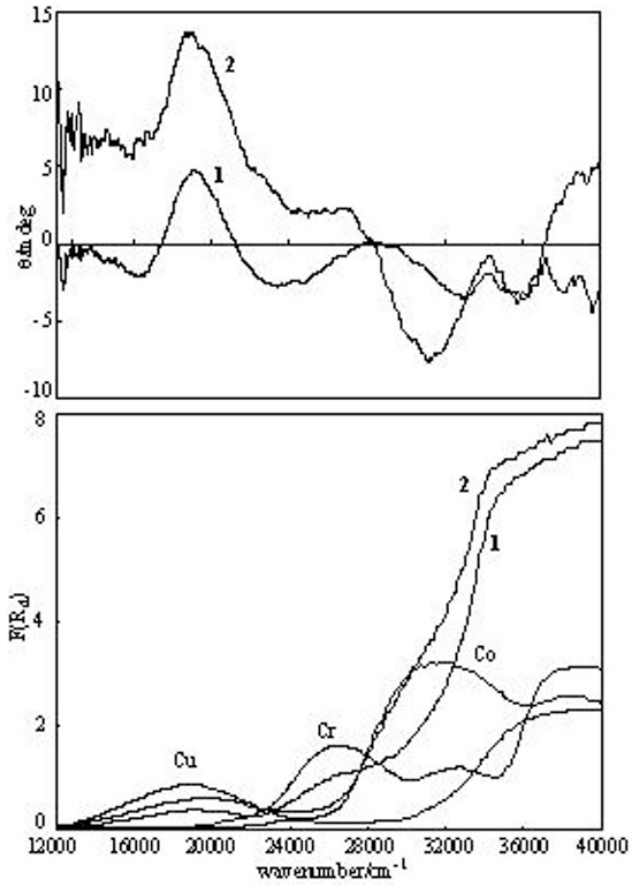


**Fig. (4).** [above] Solid state CD spectra in KBr pellets and [below] diffuse reflectance spectra of **1**, **2**, and $[Cu(chxn)_2](ClO_4)_2$ (**Cu**), $K_3[Cr(CN)_6]$ (**Cr**), and $K_3[Co(CN)_6]$ (**Co**).

44000 $cm^{-1}$ ($t_{2g}$-$t_{1u}\pi^*$), and 50000 $cm^{-1}$ ($t_{2g}$-$t_{2u}\pi^*$) for $K_3[Fe(CN)_6]$, 38600 $cm^{-1}$ ($t_{2g}$-$t_{1u}\pi^*$) for $K_3[Cr(CN)_6]$, and 49500 $cm^{-1}$ ($t_{2g}$-$t_{1u}\pi^*$) (and d-d bands at 32050 and 38460 $cm^{-1}$) for $K_3[Co(CN)_6]$. The CT bands or shoulders are also observed at 23700, and more than 28700 $cm^{-1}$ for $K_3[Fe(CN)_6]$ ($^2T_{1u}$ ground state in $O_h$ symmetry), more than 26100 $cm^{-1}$ for $K_3[Co(CN)_6]$ ($^1T_{2u}$), and 26600 $cm^{-1}$ and more than 30500 $cm^{-1}$ for $K_3[Cr(CN)_6]$ ($^4T_{2u}$).

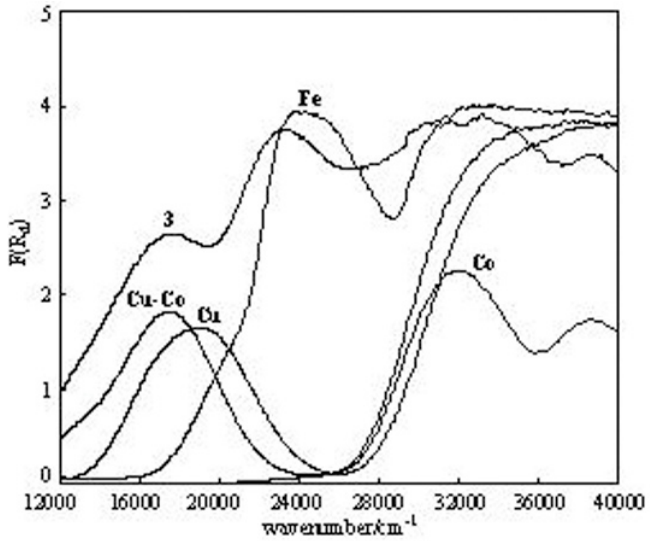


**Fig. (5).** Diffuse reflectance spectra of **3**, $[Cu(N\text{-Eten})_2]_3[Co(CN)_6]_2\cdot 4H_2O$ (**Cu-Co**), and $[Cu(N\text{-Eten})_2](ClO_4)_2$ (**Cu**), $K_3[Fe(CN)_6]$ (**Fe**), and $K_3[Co(CN)_6]$ (**Co**).

## Magnetic Properties

The temperature dependence of $\chi_M T$ values per $[Cu(chxn)_2]_3[M(CN)_6]_2\cdot 4H_2O$ or $[Cu(N\text{-Eten})_2][Fe(CN)_6]\cdot 4H_2O$ units of a powder sample of **1**-**3** measured under 0.5 T are shown in Fig. (**6**). Both **1** and **2** are composed of paramagnetic one-dimensional $Cu^{II}_2Cr^{III}_2$ chains and paramagnetic mononuclear $Cu^{II}$ moiety. At 300 K, the $\chi_M T$ value of **1** equals to 3.26 $cm^3Kmol^{-1}$, which is considerably smaller than the expected value (4.875 $cm^3Kmol^{-1}$) for uncoupled $Cu^{II}_3Cr^{III}_2$ system of $Cr^{III}$ (S = 3/2) and $Cu^{II}$ (S = 1/2). The value increases slowly with decreasing temperature down to about 40 K, then rapidly increases to reach a maximum of 7.66 $cm^3Kmol^{-1}$ at 5 K. As for **2**, the $\chi_M T$ value is 0.694 $cm^3Kmol^{-1}$ at 300 K, which is smaller than the expected value (1.625 $cm^3Kmol^{-1}$) for uncoupled $Cu^{II}_3Co^{III}_2$ system of $Co^{III}$ (S = 0) and $Cu^{II}$ (S = 1/2). As the temperature is lowered, the $\chi_M T$ value gradually increases up to 1.10 $cm^3Kmol^{-1}$ at 5 K.

On the other hand, the $\chi_M T$ value is 2.20 $cm^3Kmol^{-1}$ (4.19 B.M.) at 300 K, and it gradually increases until around 30 K, and it abruptly increases to reach up to 2.90 $cm^3Kmol^{-1}$ (4.82 B.M.) at 5 K for **3**. Which can be essentially interpret as the sum of $Cu^{II}_3Fe^{III}_2$ system, namely $\{3\mu_{eff}(Cu^{II}, S = 1/2)^2 + 2\mu_{eff}(Fe^{III}, S = 1/2)^2\}^{1/2}$ = 3.87 B.M. The unique magnetic behavior of **3** is characteristic of dominant ferromagnetic interaction upon weak antiferromagnetic interaction superimposed. In the two-dimensional chains of **3**, orthogonality of the magnetic orbitals between $Cu^{II}$ and $Fe^{III}$ ions should result in ferromagnetic predominantly, when the geometry is as it is. A low-spin $Fe^{III}$ ion in $O_h$ symmetry has the unpaired electron in degenerated $d_{xy}$, $d_{xz}$, and $d_{yz}$ ($t_{2g}^5$) orbitals of $\pi$–character, whereas axially elongated octahedral $Cu^{II}$ ions

in $D_{4h}$ symmetry have one unpaired electron in the $d_{x2-y2}$ ($b_{1g}$) orbital of σ-character.

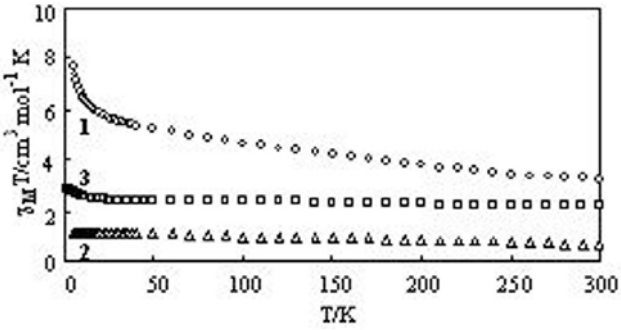


**Fig. (6).** The $\chi_M T$ vs $T$ plots at 5-300 K under 0.5 T for **1**-**3**.

### Thermally-Accessible Distortion of Different Dimensionality

The present results reveal that (1) in the one-dimensional cyanide-bridged lattices of **1** and **2**, less distorted (at room temperature) mononuclear $Cu^{II}$ moieties exhibit large structural changes induced by (cooling) temperature, (2) the less distorted $Cu^{II}$ moieties at each temperature exhibit large structural changes by changing temperature for both mononuclear $Cu^{II}$ moieties of **1** and **2** and intra-long-chain of the two-dimensional ladder structure of **3**. Indeed, the structural factors of organic ligands may be factors to determine crystal packing generally, though we limited the discussion to axial bonds of $Cu^{II}$ moieties and cell volumes for the cases of the present systems. In order to compare to other cyanide-bridged complexes having different dimensions (Fig. **7**), we can summarize only available (reported) $T$ values and cell volume data. A mononuclear complex, $[Cu(en)_2](ClO_4)_2$ (en = ethylenediamine) (Fig. **7a**), indicated $T$ = 0.780, 0.785 and 0.791 at 297, 274 and 120 K, respectively, accompanying with 2.26 % decrease of the cell volume between 297 and 120 K [42]. Diagonal one-dimensional chain, $[Cu(en)_2][Pt(CN)_4]$, showed $T$ = 0.789 at 298 K and 3.30 % decrease of the cell volume between 297 and 120 K [43]. Similar diagonal one-dimensional chain,$[Cu(N\text{-Eten})_2][Pt(CN)_4]$ (Fig. **7b**), indicated $T$ = 0.796 at 298 K [44]. However, as for these diagonal one-dimensional systems, the temperature effect is smaller than that of ionic radii by metal-substitution as shown for $[M(CN)_4]$ (M = Ni, Pd, and Pt) systems. Moreover, zigzag one-dimensional $[Cu(chxn)_2][Ni(CN)_4]\cdot 2H_2O$ (Fig. **7c**) indicated $T$ = 0.694 and 0.871 for quite long and normal axial Cu-N bonds at 297K and 1.27 % decrease of the cell volume between 297 and 120 K [45]. The lack of systematic data about various crystal packing enables us to draw more general principles at present.

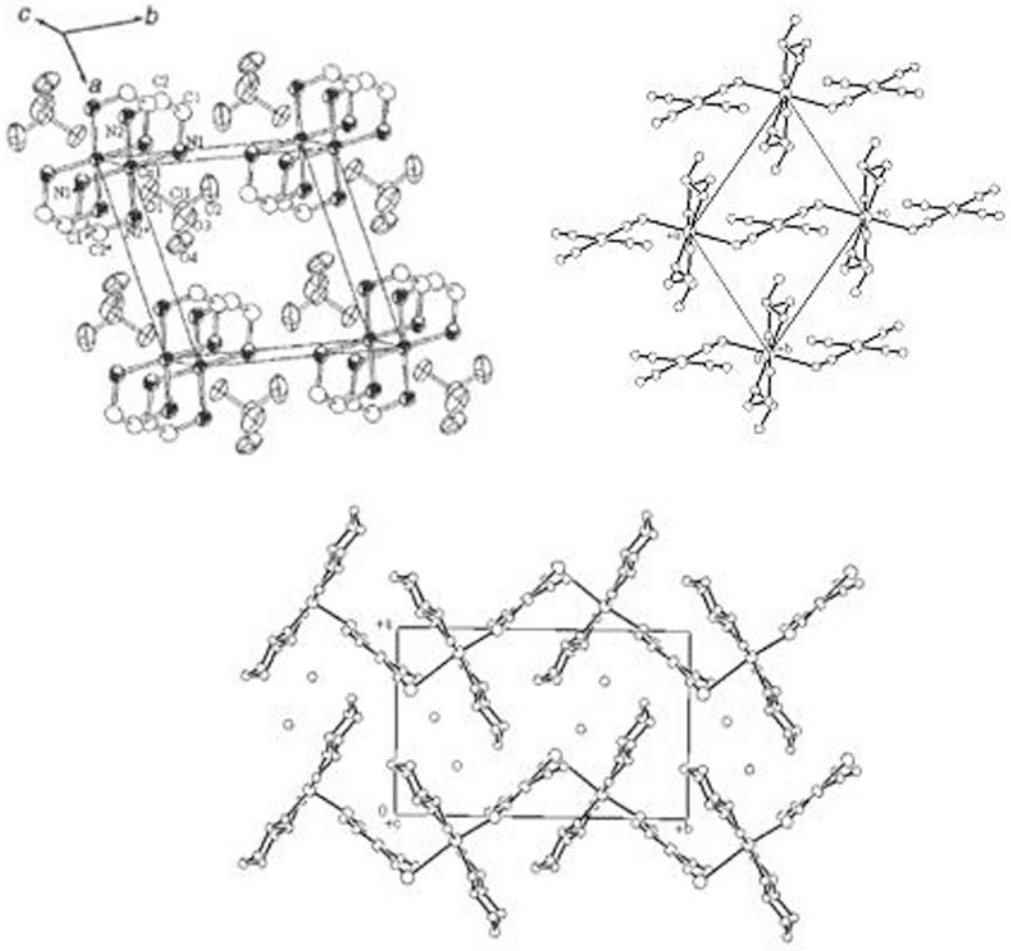


**Fig. (7).** Crystal packing schemes of (**a**) mononuclear $[Cu(N\text{-en})_2](ClO_4)_2$ [above left], (**b**) diagonal one-dimensional $[Cu(N\text{-Eten})_2][Pt(CN)_4]$ [above right], (**c**) zigzag one-dimensional $[Cu(chxn)_2][Ni(CN)_4]\cdot 2H_2O$ [below].

## Discussion

As well understood [21-23], the $Cu^{II}$ ion forms a large variety of six-coordinate complexes, and the symmetric octahedrally coordinated $Cu^{II}$ ion is subject to Jahn-Teller distortion. Even the non-symmetrically substituted $Cu^{II}$ ions or actual $Cu^{II}$ ions slightly deviated from regular polyhedrons, $Cu^{II}$ ions can exhibit pseudo Jahn-Teller distortion. Since the $Cu^{II}$ ions under such conditions are found in a wide variety of compounds and the magnitude of the Jahn-Teller effect can vary widely in actual crystal systems of low symmetry.

A question of particular interest is the cause of the structural changes that accompanies dimensionality of cyanide-bridges. The cocrystal systems of **1** and **2** may provide good examples of the way in which the interplay of Jahn-Teller vibronic coupling and crystal lattice (one-dimensional chains) forces to decide the structure adopted by the mononuclear *trans*-$[Cu^{II}L_4X_2]$ moieties. Significant deviation from regular $D_{4h}$ symmetry, namely small $T$ values, is observed for the systems exhibiting small temperature dependence of the average bond lengths. This situation may be explained as cooperative interactions between neighboring complexes. The classification of the nature of Jahn-Teller effect by $T$ values is as follows:

$T = 1.0$ --- dynamic system.

$0.9 < T < 1.0$ --- fluxional system

(temperature variable)

$T < 0.9$ --- static system

[all the present ones for **1**-**3**]

All the $Cu^{II}$ coordination spheres for the present systems are classified into $T < 0.9$, but the $Cu^{II}$ coordination spheres exhibit large thermally-accessible structural changes have small distortion with large $T$ values close to 1.0 relatively. The plasticity of $Cu^{II}$ coordination sphere and distortion isomerism may be attributed to vibronic origin modulated by crystal-packing forces and which are general features of $Cu^{II}$ complexes. However, the deviation from a regular octahedral geometry of a complex distorted by $E_g \times e_g$ Jahn-Teller coupling is described in terms of the two components $Q_\theta$ and $Q_\varepsilon$ of the Jahn-Teller active $e_g$ vibration. These vibration modes are valid for high symmetry systems. Therefore, distortion of $Cu^{II}$ coordination geometries is not determined simply by not only Jahn-Teller effect but also other factors (for example, strain caused by crystal packing and static effects by ligands) in particular low-symmetry $Cu^{II}$ environment in actual crystal lattices.

## CONCLUSION

The present results suggest that certain dimensional cyanide-bridges play an important role to determine lattice strain. And structural changes associated with Jahn-Teller distortion induced by external conditions are valid for smaller ranges than that determined by lattice strain. In other words, the larger distorted $Cu^{II}$ chromophores by Jahn-Teller effect exhibited small structural changes by low temperature for the present systems. Thus, an appropriate coordination or environment made by crystal packing forces for local structures of $Cu^{II}$ chromophores may be necessary to show structural changes by Jahn-Teller effect. Further detailed studies in view of crystal engineering are in progress now.

## ACKNOWLEDGEMENTS

This work was supported by Research Foundation for Opto-Science and Technology, Mizuho Foundation for the Promotion Science, and Iketani Science and Technology Foundation. The authors thank the Materials Design and Characterization Laboratory, Institute for Solid State Physics, the University of Tokyo for the SQUID facilities and Institute for Molecular Science for the SQUID and CCD facilities.

## REFERENCES

[1] Ohba, M.; Okawa, H. *Coord. Chem. Rev.*, **2000**, *198*, 313.
[2] Okawa, H.; Ohba, M. *Bull. Chem. Soc. Jpn.*, **2002**, *75*, 1191.
[3] Sato, O. *Acc. Chem. Res.*, **2003**, *36*, 692.
[4] Sato, O.; Hayami, S.; Einaga, Y.; Gu, Z.-Z. *Bull. Chem. Soc. Jpn.*, **2003**, *76*, 443.
[5] Sato, O.; Iyoda, T.; Fujishima, A.; Hashimoto, K. *Science*, **1996**, *272*, 704.
[6] Sato, O.; Einaga, Y.; Fujishima, A.; Hashimoto, K. *Inorg. Chem.*, **1999**, *38*, 4405.
[7] Li, G.; Akitsu, T.; Sato, O.; Einaga, Y. *J. Am. Chem. Soc.*, **2003**, *125*, 12396.
[8] Escax, V.; Champion, G.; Arrio, M.-A.; Zacchigna, M.; Cartier dit Moulin, C.; Bleuzen, A. *Angew. Chem. Int Ed.*, **2005**, *44*, 4798.
[9] Coronado, E.; Gimenez-Saiz, C.; Martinez-Agudo, J. M.; Muez, A.; Romero, F. M.; Stoeckli-Evans, H. *Polyhedron*, **2003**, *22*, 2435.
[10] Coronado, E.; Gomez-Garcia, C. J.; Nuez, A.; Romero, F. M.; Rusanov, E.; Stoeckli-Evans, H. *Inorg. Chem.*, **2002**, *41*, 4615.
[11] Coronado, E.; Gimenez-Saiz, C.; Nuez, A.; Sanchez, V.; Romero, F. M. *Eur. J. Inorg. Chem.*, **2003**, 4289.
[12] Coronado, E.; Gomez-Garcia, C. J.; Nuez, A.; Romero, F. M.; Waerenborgh, J. C. *Chem. Mater.*, **2006**, *18*, 2670.
[13] Kumagai, H.; Inoue, K. *Angew. Chem. Int. Ed.*, **1999**, *38*, 1601.
[14] Coronado, E.; Galan-Mascaros, J. R.; Gomez-Garcia, C. J.; Laukhin, V, *Nature*, **2000**, *408*, 447.
[15] Goodwin, A. L.; Chapman, K. W.; Keppert, C. J. *J. Am. Chem. Soc.*, **2006**, *127*, 17980.
[16] Pretsch, T.; Chapman, K. W.; Halder, G. J. Kepert, C. J. *Chem. Commun*., **2006**, 1857.
[17] Evans, J. S. O. *J. Chem. Soc. Dalton Trans.*, **1999**, 3317.
[18] Hathaway, B. J.; Billing, D. E. *Coord. Chem. Rev.*, **1970**, *5*, 143.
[19] Murphy, B.; Hathaway, B. J. *Coord. Chem. Rev.*, **2003**, *243*, 237.
[20] Murphy, B.; Aljabri, M.; Ahmed, A. M.; Murphy, G.; Hatahway, B. J.; Light, M. E.; Geilbrich, T.; Hursthouse, M. B. *Dalton Trans.*, **2006**, 357.
[21] Simmons, C. J. *New J. Chem.*, **1993**, *17*, 77.
[22] Falvello, L. R. *J. Chem. Soc. Dalton Trans.*, **1997**, 4463.
[23] Halcrow, M. A. *Dalton Trans.*, **2003**, 4375.
[24] Kang, D.-B. *Bull. Korean Chem. Soc.*, **2005**, *26*, 1965.
[25] Akitsu, T.; Komorita, S.; Kushi, Y. *Inorg. Chim. Acta*, **2001** *315*, 18.
[26] Akitsu, T.; Komorita, S.; Urushiyama, A. *Bull. Chem. Soc. Jpn.*, **2001**, *74*, 851.
[27] Akitsu, T.; Komorita, S.; Tamura, H. *Inorg. Chim. Acta*, **2003**, *348*, 25.
[28] Simmons, C. J.; Stratemeier, H.; Hitchman, M. A.; Riley, M. J. *Inorg. Chem.*, **2006**, *45*, 1021.
[29] Schultz, A. J.; Henning. R. W.; Hitchman, M. A.; Stratemeier, H. *Cryst. Growth. Des.*, **2003**, *3*, 203.
[30] Chen, Z.; Fei, S.; Strauss, H. L. *J. Am. Chem. Soc.*, **1998**, *120*, 8789.
[31] Wijnangs, P. E. M.; Wood, J. S.; Reedijk. J.; Maaskant, W. J. A. *Inorg. Chem.*, **1996**, *35*, 1214.
[32] Akitsu, T.; Einaga, Y. *Acta Crystallogr. Sect. E*, **2006**, *62*, 750.
[33] Sheldrick, G. M. SHELXL-97, University of Gottingen: Germany, 1997.
[34] Pariya, C.; Liao, F.-L.; Wang, S.-L.; Chung, C.-S. *Polyhedron*, **1998**, *17*, 547.

[35] You, Y. S.; Yoon, J. H.; Lim, J. H.; Kim, H. C.; Hong, C. S. *Inorg. Chem.*, **2005**, *44*, 7063.
[36] Ohkoshi, S.; Tokoro, H.; Hozumi, T.; Zhang, Y.; Hashimoro, K.; Mathoniere, C.; Bord, I.; Rombaut, G.; Verelst, M.; Cartier dit Moulin, C.; Villain, F. *J. Am. Chem. Soc.*, **2006**, *126*, 270.
[37] Hozumi, T.; Nuida, T.; Hashimoto, K.; Ohkoshi, S. *Cryst. Growth Des.*, **2006**, *6*, 1736.
[38] Lim, J. H.; Kang, J. S.; Kim., H. C.; Koh, E. K.; Hong, C. S. *Inorg. Chem.*, **2006**, *45*, 7821.
[39] Larionova, J.; Clerac, R.; Fonnadieu, B.; Eillemin, S. Guerin, C. *Cryst. Growth Des.*, **2003**, *3*, 267.
[40] Mukhopadhyay, U.; Bernal, I. *Cryst. Growth Des.*, **2005**, *5*, 363.
[41] Mukhopadhyay, U.; Bernal, I. *Cryst. Growth Des.*, **2005**, *5*, 1687.
[42] Akitsu, T.; Einaga, Y. *Bull. Chem. Soc. Jpn.*, **2004**, *77*, 763.
[43] Akitsu, T.; Einaga, Y. *Acta Crystallogr. Sect. E*, **2006**, *62*, 862.
[44] Akitsu, T.; Einaga, Y. *Inorg. Chim. Acta*, **2007**, *360*, 497.
[45] Akitsu, T.; Einaga, Y. *Inorg. Chem.*, **2006**, *35*, 9826.

Received: November 07, 2007 Revised: December 07, 2007 Accepted: December 07, 2007